

## Adsorption of phenanthrene on activated carbon increases mineralization rate by specific bacteria

Pierre Leglize<sup>a</sup>, Saada Alain<sup>b</sup>, Berthelin Jacques<sup>a</sup>, Leyval Corinne<sup>a,\*</sup>

<sup>a</sup> *Laboratoire des Interactions Microorganismes, Minéraux, Matière Organique dans les Sols (LIMOS) UMR 7137 CNRS-UHP Nancy I, Faculté des Sciences, BP 239, F54506 Vandoeuvre-lès-Nancy Cedex, France*

<sup>b</sup> *Bureau de Recherches Géologique et Minière (BRGM), Division Environnement et procédés, 3 rue Claude Guillemin, F45060 Orléans Cedex 2, France*

Received 3 July 2006; received in revised form 28 May 2007; accepted 29 May 2007

Available online 7 June 2007

### Abstract

Bioavailability of polycyclic aromatic hydrocarbons (PAH) in soil is affected by PAH sorption to solid phase. We studied the influence of activated carbon (AC) on phenanthrene (PHE) mineralization by five degrading bacterial strains isolated from contaminated soil. PHE adsorption on AC was important and reduced PHE aqueous concentration up to 90%. PHE degradation was improved in the presence of activated carbon with three of the bacterial strains, named NAH1, MATE3 and MATE7, which produced biofilms, whereas it was not improved with the two other ones, which did not produce biofilms, MATE10 and MATE12. Monitoring PHE distribution during incubation showed that aqueous PHE concentration was significantly higher with the biofilm-producing NAH1 than with MATE10. Bacterial adhesion on AC was also investigated. The pre-coating of AC with PHE increased NAH1 and MATE3 adhesion to the solid surface (>16 and >13%, respectively). Bacterial properties, such as biofilm production and adhesion to AC capacity seemed to be related to their ability to optimize PHE degradation by improving PHE diffusion and reducing diffusion path length.

© 2007 Elsevier B.V. All rights reserved.

**Keywords:** PAH; Biodegradation; Biofilm; Activated carbon; Bacterial adhesion

### 1. Introduction

The fate of polycyclic aromatic hydrocarbons (PAH) in soil and groundwater is of great environmental concern due to their carcinogenic properties and their persistence due to low solubility and bioavailability. PAH contaminant sources include petroleum, oil or creosote loss from storage facilities and incomplete combustion of organic matter, such as fossil fuels or wood. Soil and groundwater bioremediation methods have gained attention over the last decades.

Microorganisms are the major agents mineralizing PAH in terrestrial environments [1], either directly as carbon source or via co-metabolism, when they use another substrate for growth [2,3]. PAH have a strong tendency to adsorb onto solid surfaces

especially hydrophobic sites. A reduction in water concentration due to adsorption can modify the accessibility and bioavailability of PAH [4] and then decrease [4,5] or enhance [6,7] their biodegradation.

Microbial degrading efficiency of potential substrates that are bound to particles seems to be strain dependant [8–10]. Physiological properties of PAH-degrading strains contribute to promote PAH degradation, through mechanisms including: (i) efficient adhesion capacity to hydrophobic surfaces [7], (ii) increase of the diffusive substrate flux [11] and (iii) production of surfactants or biofilms [12–14].

Biofilm formation by bacteria is often a stress response to harmful conditions and plays a key role in initial adherence of bacteria to solid surfaces [15]. Eriksson et al. [14] reported growth of bacterial biofilm directly on pyrene crystal and observed an important pyrene removal rate. Rodrigues et al. [16] showed that *Pseudomonas putida* ATCC 17514 was able to utilize phenanthrene at a higher rate than fluorene by forming biofilm on phenanthrene surface and not on fluorene. Guieysse et al. [17] showed that biofilmed reactors were

\* Corresponding author. Tel.: +33 383684282; fax: +33 383684284.

E-mail addresses: [pierre.leglize@limos.uhp-nancy.fr](mailto:pierre.leglize@limos.uhp-nancy.fr) (P. Leglize), [a.saada@brgm.fr](mailto:a.saada@brgm.fr) (S. Alain), [jacques.berthelin@limos.uhp-nancy.fr](mailto:jacques.berthelin@limos.uhp-nancy.fr) (B. Jacques), [corinne.leyval@limos.uhp-nancy.fr](mailto:corinne.leyval@limos.uhp-nancy.fr) (L. Corinne).

efficient for the bioremediation of PAH-contaminated groundwater.

Activated carbon (AC) seems to be a good adsorbent to remove organic pollutant from groundwater due to its high adsorption capacity and has been proposed for permeable reactive barrier technique [18]. A previous study [19] has shown that the presence of AC improved PHE mineralization by a *Burkholderia* sp. strain compared to treatment without AC.

The objective of this work was to study the effect of AC on phenanthrene (PHE) mineralization in batch experiments with five PAH-degrading strains forming or not biofilm. In addition, PHE distribution in reactors during biodegradation experiment was examined. Sorption of PHE on AC, as well as adhesion of the PAH-degrading bacteria on AC and on AC covered with PHE were estimated.

## 2. Materials and methods

### 2.1. Materials

Phenanthrene (PHE) was used as model PAH. The stock solutions of PHE were prepared in methanol (HPLC grade, Carlo Erba) from labelled  $^{14}\text{C}_9$ -PHE (98% purity, specific activity  $30.34 \times 10^7 \text{ Bq mmol}^{-1}$ , Sigma) and non-labelled PHE (98% purity, Sigma).

The adsorbent used in the experiments was a commercial activated carbon (AC) (PICA, France) with a particle size ranging between 0.85 and 1.1 mm.

PHE-degrading bacterial strains were isolated from PAH-contaminated soils of a former gas works site in France using a procedure described by Binet et al. [20]. Only purified bacterial isolates that were able to degrade PHE as only carbon source and kept their ability to degrade PHE after a subculture without PHE were used. Five isolates were selected, referred to as NAH1, MATE3, MATE7, MATE10 and MATE12. The five isolates were gram-negative bacteria. Three of them formed biofilms on agar plates and in liquid media (NAH1, MATE3 and MATE7). The isolates were identified, based on the partial sequence of 16S rDNA (primer sets 968f 1401r, 475 pb [21]) (ABBioGen) as *Burkholderia* sp. (AY178099, 100% homology), *P. putida* (AE016778, 99% homology), *Achromobacter xylosoxidans* (AY189752, 100% homology), *S. maltophilia* (AY445079, 99% homology) and *S. maltophilia* (AT367030, 99% homology), respectively.

### 2.2. Methods

#### 2.2.1. Bacterial culture and biofilm formation

All strains were maintained as liquid culture in Bushnell Hass (BH,  $3.27 \text{ g l}^{-1}$ ) medium with PHE ( $200 \text{ mg l}^{-1}$ ) as the only carbon source. In order to have enough biomass, the isolates ( $20 \mu\text{l}$  of liquid culture) were pre-incubated for 48 h in 5 ml of Luria–Bertani Broth (LB) medium (peptone,  $10 \text{ g l}^{-1}$ ; yeast extract,  $5 \text{ g l}^{-1}$ ; NaCl,  $5 \text{ g l}^{-1}$ ) before each experiment. Cells were then washed twice with sterile NaCl solution ( $8.5 \text{ g l}^{-1}$ ) before used. Biofilm formation was observed first on Petri

plate cultures (Bushnell Hass medium, Difco,  $3.27 \text{ g l}^{-1}$ ; agar,  $15 \text{ g l}^{-1}$ ; PHE,  $300 \text{ mg l}^{-1}$ ) and in experimental flasks (mucoids surrounded AC). It was confirmed by scanning confocal laser microscopy (SCLM) observations on AC particles sampled at the end of the mineralization experiments (see Sections 2.2.5.1 and 2.2.5.2). Bacterial cells were stained using LIVE/DEAD BacLight<sup>®</sup> Bacterial viability kit (Molecular probes) and the method provided by the manufacturer. Biofilm was stained using acridine orange (AO) buffer as described by Moller et al. [22]. SCLM observations were performed on a Biorad confocal laser microscope (Radiance 2100) with a Nikon optic (TE2000 U Eclipse, 20X). AC surface, bacterial cells and biofilm were visualized simultaneously using the Argon 488- and 514-nm line (for bacterial cells and biofilm) and the red laser diode 637-nm line (for AC reflection).

#### 2.2.2. Activated carbon (AC) characterization

BET surface areas ( $S$ ,  $\text{m}^2 \text{ g}^{-1}$ ) were determined from  $\text{N}_2$  adsorption isotherm data collected at 77 K. External area of the matrices ( $S_e$ ,  $\text{m}^2 \text{ g}^{-1}$ ) was estimated using the  $t$ -plot method [23] from  $\text{N}_2$  adsorption isotherm data. The  $t$ -plot method consists in drawing the adsorbed volume ( $\text{cm}^3 \text{ g}^{-1}$ ) at a given relative pressure  $P/P_0$ , as a function of the statistical width  $t$  ( $\text{\AA}$ ) of the adsorbed layer on a non-porous reference sample, at the same relative pressure. Mercury porosimetry was carried out up to 206 MPa (Micrometrics Pore Sizer 9310) from which the volumes of pores with diameter between 3.6 and 50 nm (mesoporosity-Vme), greater than 50 nm (macroporosity-Vma) and  $1 \mu\text{m}$  (Vb) were obtained. IUPAC recommendations [24] were used for the size definition of meso- and macro-pores. We checked that AC did not contain PAH (data not shown).

#### 2.2.3. Sorption of phenanthrene (PHE) on AC

The adsorption isotherms of PHE on AC were obtained with an aqueous solution ( $10^{-3} \text{ M CaCl}_2$ ) composed of a mixture of non-labelled and  $^{14}\text{C}_9$ -labelled PHE (10% of labelled PHE) using a procedure described by Gaboriau and Saada [25]. Adsorption isotherms were performed with 50 mg AC and 50 ml of PHE solution at  $21 \pm 2^\circ\text{C}$ . The aqueous solutions were prepared from methanol stock solution of PHE diluted in an aqueous solution of  $10^{-3} \text{ M CaCl}_2$  so that (i) PHE concentration was between 60 and  $400 \mu\text{g l}^{-1}$ , (ii) methanol concentration was less than 1%, (iii) activities ranged between 0.7 and  $1.7 \cdot 10^8 \text{ Bq l}^{-1}$ . Solution activity was measured by liquid scintillation counting on 1 ml of solution mixed with 10 ml of Ultimagold<sup>®</sup> (Perkin-Elmer) on a Tricarb 1900CA (Perkin-Elmer). The contact time between the PHE solution and AC was 48 h [19]. Glass tubes closed by Teflon stoppers were used for all experiments. The adsorption isotherm was described by a non-linear isotherm of the Freundlich type:

$$Q_{\text{ads}} = K_f \times C_{\text{eq}}^n$$

$Q_{\text{ads}}$  is the quantity of PHE adsorbed ( $\mu\text{g kg}^{-1}$ ),  $C_{\text{eq}}$  the equilibrium aqueous concentration ( $\mu\text{g l}^{-1}$ ),  $K_f$  the Freundlich adsorption coefficient ( $\mu\text{g kg}^{-1}/(\mu\text{g l}^{-1})^n$ ), and  $n$  is the energy heterogeneity of the adsorption site.

After adsorption, desorption was performed at the highest initial PHE concentration by three successive replacements of the solution (25 ml) with aqueous solution of  $10^{-3}$  M  $\text{CaCl}_2$  without PHE. Flasks were rotary stirred for 48 h between two replacements of the solution. Solution activity was measured as described above. The amount of PHE desorbed from each desorption step was calculated from the difference in solution-phase concentration during consecutive steps.

#### 2.2.4. Bacterial adhesion on AC and AC covered with PHE (ACPHE)

ACPHE was prepared as follows: 50 ml of PHE solution ( $1 \text{ mg l}^{-1}$  into BH medium,  $3.27 \text{ g l}^{-1}$ ) were stirred for 24 h on a rotary stirrer. Twenty milligrams of AC were then added and the tubes were stirred again for 48 h to allow equilibration. ACPHE was collected aseptically and dried for 2 h under a laminar flow hood at room temperature to reduce PHE volatilization losses. Bacterial cells were pre-cultivated and rinsed as described above. Three milliliters ( $\text{NaCl}$ ,  $8.5 \text{ g l}^{-1}$ ) of cell suspension ( $5.10^7 \text{ cells ml}^{-1}$ ) were incubated with increasing quantity of AC or ACPHE (1–100 mg) on a rotary stirrer for 1 h. Bacteria were then counted in the liquid phase using Thoma Cell (Preciss, VWR).

#### 2.2.5. PHE mineralization

**2.2.5.1. Effect of AC on PHE mineralization.** PHE mineralization was studied in batch with or without AC in aerobic conditions. One hundred milliliter-flasks contained 50 ml of an aqueous PHE solution, as the carbon source, prepared from methanol stock solution of PHE diluted in a mineral medium (BH,  $3.27 \text{ g l}^{-1}$ ) so that PHE concentration was  $1 \text{ mg l}^{-1}$  and the percentage of methanol was less than 1%. PHE concentration was chosen so that concentration would be below its aqueous solubility. Flasks were rotary stirred for 24 h in a dark incubation room at  $28^\circ\text{C}$ . Twenty milligrams of AC were then added and the flasks were stirred again for 48 h. Bacterial cells (NAH1, MATE3, MATE7, MATE10 or MATE12), pre-cultivated and rinsed as above, were inoculated so that bacterial concentration was  $10^6 \text{ cells ml}^{-1}$ . Abiotic (non-inoculated) controls with or without AC were included. All treatments were performed in triplicate. PHE mineralization was monitored by total  $\text{CO}_2$  measurements. Preliminary controls were performed to check that methanol mineralization was not significant and that AC was not a carbon source for bacteria. Periodically, a 10 ml portion of the flask headspace was sampled with a syringe and analyzed for  $\text{CO}_2$  content (Binos infrared spectrophotometer; absorption at  $2325.6 \text{ cm}^{-1}$ ). Flasks headspace was then changed under a laminar flow hood for 15 min to renew the air.

**2.2.5.2. PHE distribution in batch experiment with two bacterial strains forming or not biofilm.** A  $^{14}\text{C}$ -labelled PHE mineralization experiment was performed in batch with or without AC. One hundred milliliter-flasks contained 50 ml of an aqueous PHE solution prepared from methanol stock solution of labelled and non-labelled PHE (5% of labelled PHE)

diluted in a mineral medium (Bushnell Hass, Difco) so that PHE concentration was  $1 \text{ mg l}^{-1}$ , the percentage of methanol was less than 1%, and the activity was  $10^8 \text{ Bq l}^{-1}$ . Flasks were rotary stirred for 24 h in a dark incubation room at  $28^\circ\text{C}$ . Initial solution activity was then measured by liquid scintillation counting of 1 ml of solution mixed with 10 ml of Ultimagold® (Perkin-Elmer) on a Tricarb 1900CA (Perkin-Elmer). Twenty milligrams of AC were then added and the flasks were stirred again for 48 h. Solution activity was then measured and the amount of adsorbed PHE onto media was deduced from the difference in solution activity. Bacterial cells, pre-cultivated and rinsed as above, were inoculated so that bacterial concentration was  $10^6 \text{ cells ml}^{-1}$ . Two bacterial strains, producing biofilms (NAH1) or not (MATE10), were used. Abiotic (non-inoculated) controls with or without AC were included and prepared as described above. There were three replicates for each treatment.  $^{14}\text{C}$ -PHE mineralization was studied by monitoring the  $^{14}\text{CO}_2$ . A flow of decarbonated air ( $\sim 50 \text{ ml min}^{-1}$ ) was used to purge the  $^{14}\text{CO}_2$  from the headspace of the batch for 45 min and the displaced gasses were bubbled through 10 ml  $\text{NaOH}$  solution (0.4N) in order to trap  $^{14}\text{CO}_2$ .  $\text{NaOH}$  solution activity was measured by liquid scintillation counting as described above.  $^{14}\text{CO}_2$  was monitored twice a week. Once a week PHE concentration in solution and amount of PHE adsorbed onto AC were monitored. PHE concentration in solution was deduced from the solution activity measured by liquid scintillation. Activity adsorbed onto AC was extracted with dichloromethane. Preliminary extraction experiments were performed to establish solid/liquid ratio and extraction duration (data not shown). A glass tube was filled with between 10 and 15 mg of AC mixed with 20 ml of dichloromethane. The samples were shaken for 30 min on a rotary stirrer. Solvent solution activity was measured by liquid scintillation counting as described above. Bacterial cells in suspension were monitored by direct counting using Thoma Cell (VWR).

#### 2.2.6. Statistics

For each experiment, statistical differences between treatments (with or without AC, AC covered or not with PHE, with different bacterial strains) were determined by Kruskal–Wallis ANOVA on ranks using Sigmastat 3.11 software (Sysstat software). Non-parametric Student–Newman–Keuls test ( $p \leq 0.05$ ) was used to compare treatment means.

### 3. Results

#### 3.1. AC and ACPHE characterization

AC surface area was very high (Table 1). Adsorption of PHE on AC reduced BET surface area ( $>20\%$ ), possibly by reducing the surface area available for  $\text{N}_2$  molecules, but did not affect micropore area fraction (98%). Hg porosimetry showed that PHE adsorption on AC did not affect porosity distribution (data not shown) but reduced total porosity by 40% and the volume of pores with diameter greater than  $1 \mu\text{m}$  by 42% (Table 1).

Table 1  
BET surface area and pores volumes obtained from Hg porosimetry of activated carbon coated (ACPHE) or not (AC) with phenanthrene

	BET surface area (m <sup>2</sup> /g)	Micropore area (m <sup>2</sup> /g)	Total porosity (cm <sup>3</sup> /g)	Vme (3.6–50 nm) (cm <sup>3</sup> /g)	Vma (>50 nm) (cm <sup>3</sup> /g)	Vb (>1 μm) (cm <sup>3</sup> /g)
AC	1347.17	1319.13	0.359	0.129	0.230	0.147
ACPHE	1044.59	1019.86	0.214	0.071	0.143	0.084

### 3.2. PHE adsorption on AC

The adsorption of PHE on AC was described by a non-linear isotherm of Freundlich type. Freundlich adsorption coefficients showed that AC had a high PHE adsorption capacity ( $K_f = 12578 (\mu\text{g kg}^{-1}/(\mu\text{g l}^{-1}))^n$ ). At each desorption step, PHE desorption from AC was limited, up to 2% of adsorbed PHE.

### 3.3. Bacterial adhesion on AC and AC covered with PHE

Bacterial adhesion on AC was similar for all tested isolates, reaching 64–66% of the initial number of cells in suspension for 100 mg of AC (Fig. 1). No bacterial adhesion on glassware was observed (data not shown). PHE adsorption on AC significantly improved adhesion of NAH1 and MATE3 for all tested

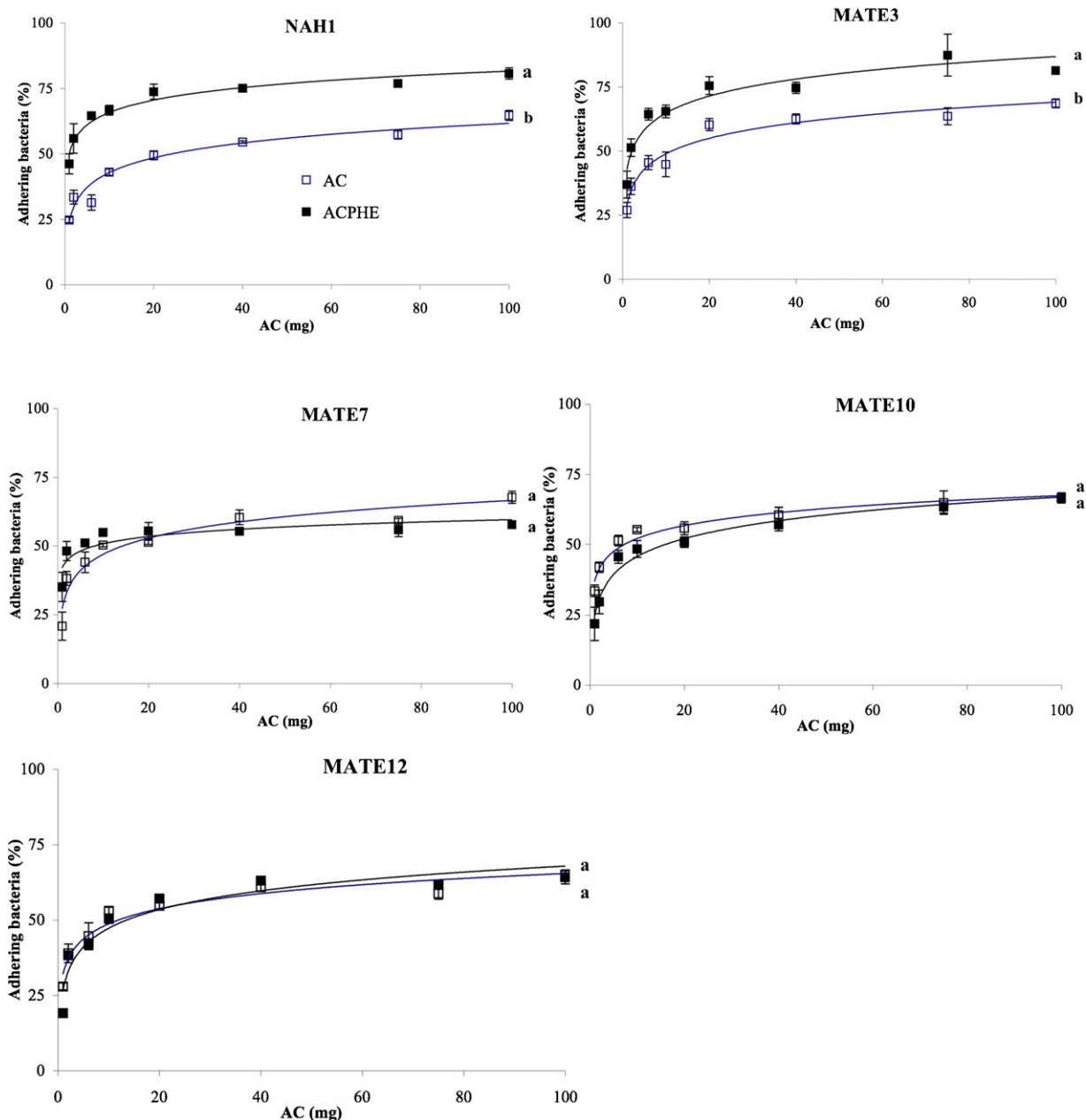


Fig. 1. Bacterial adhesion on activated carbon coated (ACPHE) or not (AC) with phenanthrene. Mean and standard error ( $n=3$ ), different letters indicate significant difference ( $p \leq 0.05$ ) between AC and ACPHE within one strain.

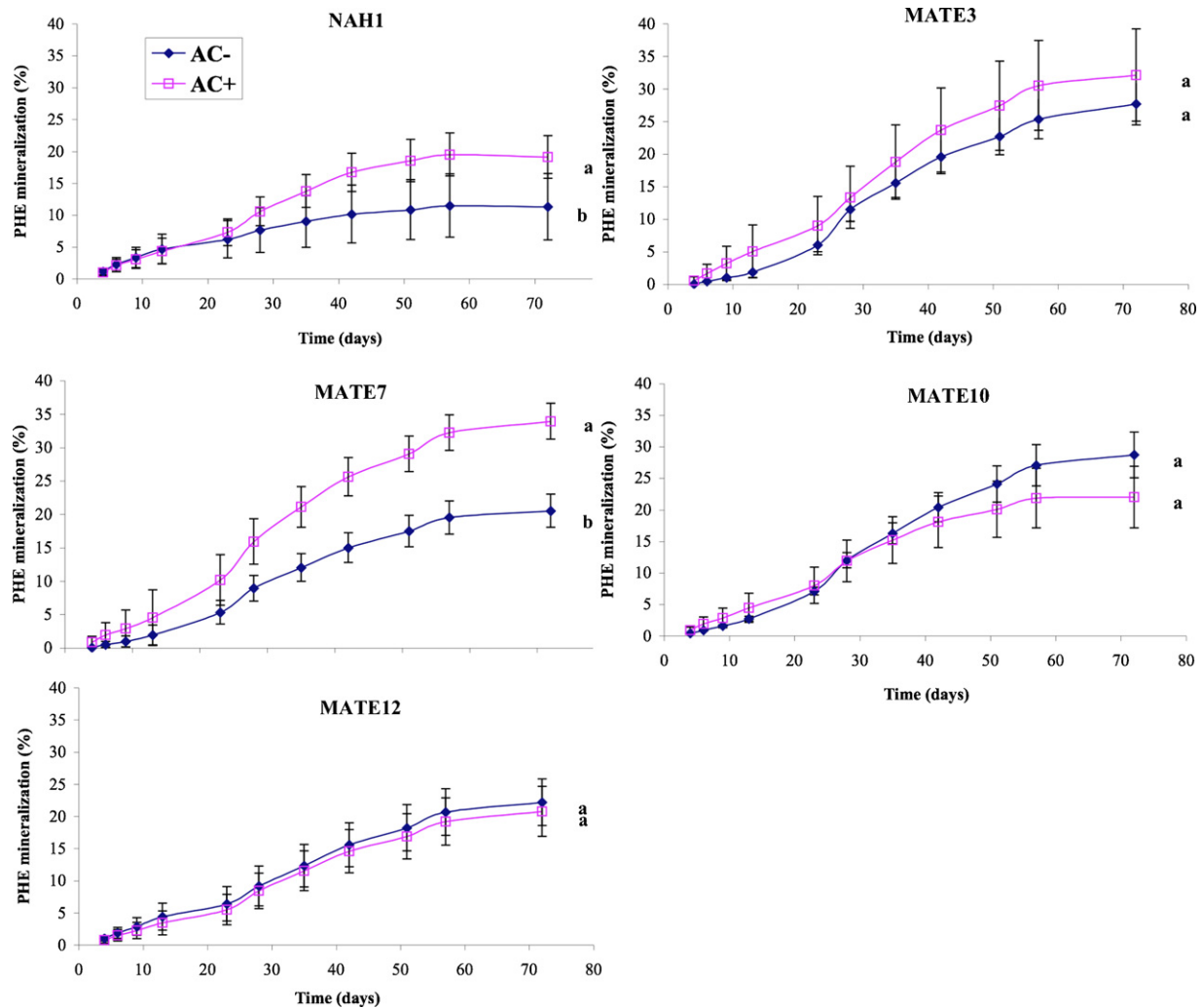


Fig. 2. Phenanthrene mineralization in batch reactor with (AC+) or without activated carbon (AC-). Mean and standard error ( $n=3$ ). Different letters indicate significant difference ( $p \leq 0.05$ ) between AC- and AC+ within one strain at the end of the experiment.

quantities of AC. For MATE7, a positive effect of PHE on bacterial adhesion to AC was observed with few quantities of AC (<20 mg). No effect was observed for MATE10 and MATE12.

### 3.4. Effect of AC on PHE mineralization

Batch experiments with non-labelled PHE showed little abiotic mineralization, less than 5% in abiotic controls with or without AC that was deduced from the data in Fig. 2. With MATE7, PHE mineralization rate was significantly ( $p \leq 0.05$ ) higher with than without activated carbon from the beginning till the end of the experiment, while with NAH1 it was significantly ( $p \leq 0.05$ ) higher only after 28 days. Without AC, the highest mineralization rate after 72 days was obtained with MATE10 ( $29 \pm 3.6\%$ ), and with MATE7 in presence of AC ( $34 \pm 2.7\%$ ). The lowest PHE mineralization rate was obtained with NAH1 with ( $19 \pm 3.3\%$ ) or without AC ( $11 \pm 5.2\%$ ). For NAH1 and MATE7, PHE mineralization significantly increased ( $p \leq 0.05$ ) in presence of AC. With MATE3, PHE mineralization also tended to be higher in presence of AC, but the difference was not significant. No difference in PHE mineralization with

or without AC was observed for MATE12. For MATE10, the presence of AC tended to reduce PHE mineralization but this was not significant.

### 3.5. PHE distribution in batch experiment with two bacterial strains forming or not biofilm

The PHE mineralization experiment with labelled PHE was interrupted after 29 days since no PHE mineralization was observed between day 19 and day 29. Up to 14% (NAH1 AC-) and 29% (MATE10 AC-) of PHE was degraded after 29 days (Table 2). Control vials with or without AC and no bacteria showed little abiotic degradation (less than 2.5%, data not shown) that was deduced from the data in Table 2. The PHE mineralization rates differed in the labelled experiment in comparison to the experiment with non-labelled PHE, possibly due to different aeration conditions. However, the former experiment confirmed that PHE mineralization was higher with MATE10 than with NAH1 without AC ( $p \leq 0.05$ ) and that the presence of AC significantly ( $p \leq 0.05$ ) increased PHE mineralization by NAH1. In this experiment, PHE mineralization significantly

Table 2  
 $^{14}\text{C}$ -PHE mineralization by NAH1 or MATE10 with (AC+) or without activated carbon (AC–), PHE adsorption on AC and PHE in solution during the same experiment

Times (days)	NAH1		MATE10	
	AC– (% mineralized PHE)	AC+ (% mineralized PHE)	AC– (% mineralized PHE)	AC+ (% mineralized PHE)
1	0.1 ± 0.0 aA	1.0 ± 2.9 aA	0.1 ± 0.0 aA	0.1 ± 0.0 aA
8	10.2 ± 2.2 aA	19.4 ± 9.4 bA	16.3 ± 1.8 aB	8.8 ± 5.5 bA
15	12.6 ± 2.8 aA	23.0 ± 8.5 bA	28.5 ± 4.5 aB	24.0 ± 4.0 aA
29	14.2 ± 3.1 aA	25.5 ± 12.8 bA	28.8 ± 4.5 aB	26.3 ± 3.7 aA

Times (days)	NAH1		MATE10	
	% Adsorbed PHE	% PHE in solution	% Adsorbed PHE	% PHE in solution
1	87.9 ± 3.3 A	2.1 ± 0.8 A	80.0 ± 9.6 A	2.6 ± 0.3 A
8	59.5 ± 7.2 A	2.2 ± 0.3 A	73.2 ± 14.2 A	1.5 ± 1.2 A
15	54.9 ± 2.8 A	3.0 ± 1.6 A	53.8 ± 10.3 A	1.5 ± 0.5 B
29	51.7 ± 1.3 A	2.2 ± 0.7 A	53.5 ± 3.0 A	1.1 ± 0.4 B

Mean and standard error ( $n=3$ ); different small letters (a, b) indicate significant differences ( $p \leq 0.05$ ) between AC– and AC+ within one strain; different capital letters (A, B) indicate significant differences ( $p \leq 0.05$ ) between bacterial strains within one parameter.

decreased ( $p \leq 0.05$ ) in presence of AC for MATE10. At the beginning of the experiment, most of the added PHE was sorbed to AC (78%) and initial PHE concentration in solution was less than  $50 \mu\text{g l}^{-1}$  (4%) (Table 2). Percentage recovery of  $^{14}\text{C}$  ranged between 80 and 90%, suggesting losses via adsorption on batch components (glass tubes). PHE concentration in solution significantly decreased after inoculation with MATE10 and NAH1, but it decreased more with MATE10 (up to 1.1%) than with NAH1 (up to 2.2%). PHE concentration in solution was significantly higher for NAH1 than MATE10 after 15 days. In presence of AC, the number of suspended bacteria decreased during the first 5 days (Fig. 4). The reduction was significantly more pronounced for NAH1 than MATE10. The number of suspended bacteria increased similarly with or without media and with NAH1 or MATE10 after 5 days.

### 3.6. Bacterial distribution on AC surface and biofilm production

At the end of the experiment with non-labelled PHE, spatial distribution of NAH1, MATE3 and MATE7 was similar with dense cell clusters embedded in biofilms, whereas MATE10 and MATE12 were homogeneously distributed on the AC surface (Fig. 3). The same distributions were observed with NAH1 and MATE10 at the end of the experiment with labelled PHE (data not shown).

## 4. Discussion

The five strains were related to soil bacteria involved in organic contaminant biodegradation. NAH1 was used by Amelal et al. [26] in order to study PAH bioavailability within soil aggregates. MATE3 was closely related to *P. putida* species previously studied for soil naphthalene degradation [27,28]. Cutright and Lee [29] have shown that *Achromobacter* sp. is able to degrade PAH. MATE10 and MATE12 strains were related to *Stenotrophomonas maltophilia* sp. which were previously studied by Boochan et al. [30] or Juhasz et al. [31] for high molecular weight PAH microbial degradation and detoxification.

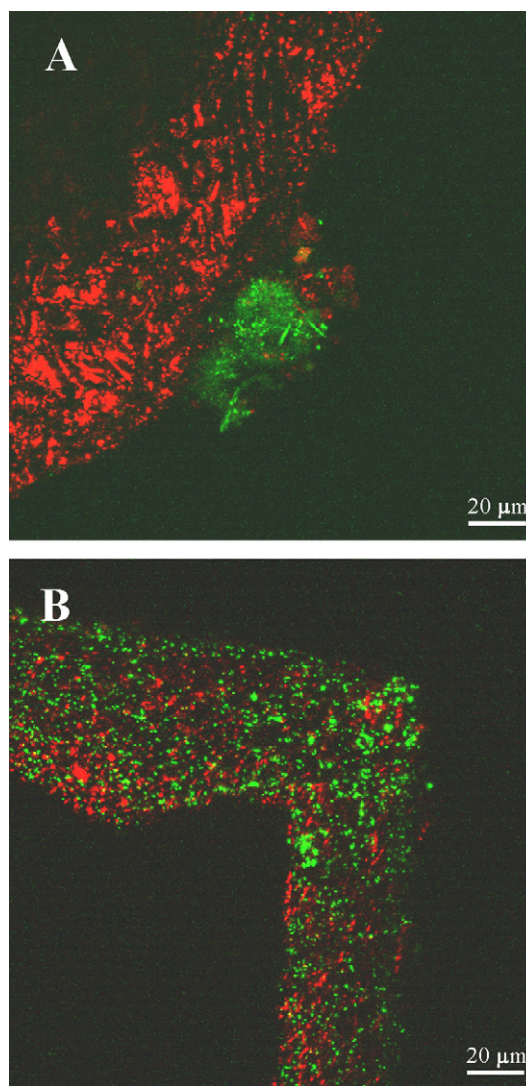


Fig. 3. Scanning confocal observations of NAH1 (A) and MATE10 (B) bacterial strains on activated carbon particles after 72 days of incubation. Bacteria were stained with a LIVE/DEAD kit (green), biofilm was stained with AO buffer (green) and AC surface was obtained from helium–neon reflection (red).

Activated carbon characterization (Table 1) showed a large reactive surface, which could explain its high phenanthrene adsorption capacity. The presence of activated carbon reduced PHE concentration in solution by up to 90% (Table 1). Decreased PAH solution concentration can reduce their bioavailability [32]. However, for all tested strains, the presence of activated carbon did not reduce phenanthrene mineralization. With MATE10 and MATE12, PHE mineralization rate was similar with or without AC. This suggests, as previously observed with a mixed culture of PHE degraders by Laor et al. [33] that these two strains were able to use PHE from the bound phase and at the same rate as from the free phase. With NAH1, MATE3 and MATE7, the presence of AC increased PHE mineralization rate (+19, +16 and +29%, respectively). These three isolates formed biofilms while the others did not. For all strains, in presence of AC, PHE mineralization rate was higher (MATE10,  $0.28 \pm 0.09 \mu\text{g day}^{-1}$ ; MATE7,  $0.38 \pm 0.14 \mu\text{g day}^{-1}$ ) than PHE desorption rate ( $0.14 \mu\text{g day}^{-1}$ ) calculated from the adsorption–desorption experiment. The increased mineralization rate of PHE adsorbed on AC could be related to physiological properties of the three isolates, which formed biofilms. NAH1, MATE3 and MATE7 had higher adhesion capacity on AC coated with PHE than the other isolates (Fig. 1) and their adhesion on ACPHE was higher than on AC. These three strains may have direct access to phenanthrene adsorbed on activated carbon. Attached bacteria are often more active than free cells. Moreno-Castilla et al. [34] have shown that adhesion of *Escherichia coli* on AC improved water denitrification process. Other authors have shown the direct utilization of sorbed pollutants by microorganisms attached to the solid [11,35]. Harms and Zehnder [11] have demonstrated that degradation of 3-chlorodibenzofuran sorbed to Teflon was facilitated by microbial adherence. Attached cells transformed the desorbing 3-chlorodibenzofuran within a short distance from the sorbent, creating a steep concentration gradient. This gradient affected the rate of desorption which was then not only driven by the chemical partitioning between the water phase and the solid phase [7]. Our results are in agreement with Poeton et al. [6], who have shown that phenanthrene biodegradation rate by marine bacteria was higher in the presence than in the absence of sediment at the same aqueous phenanthrene concentration. They gave two explanations: (i) treatment with sediment contained more phenanthrene than treatment without sediment so that more phenanthrene was available from the solid phase and (ii) more bacteria were sorbed to sediment surface when phenanthrene was adsorbed to it. In our experiment, the first explanations could not be applied because the amount of added PHE was the same with or without AC.

Biofilm formation by the three bacterial strains, NAH1, MATE3 and MATE7, may be involved in their higher ability to degrade PHE adsorbed on AC. These biofilms consisted of cell aggregates embedded in extracellular matrices. This extracellular matrix mainly contain organic molecules, such as complex glucides or fatty acids [36,37] which may act as biosurfactants, and improve PHE solubility and desorption from activated carbon. Johnsen et al. [38] have demonstrated that biological and physico-chemical factors influence PAH microbial degra-

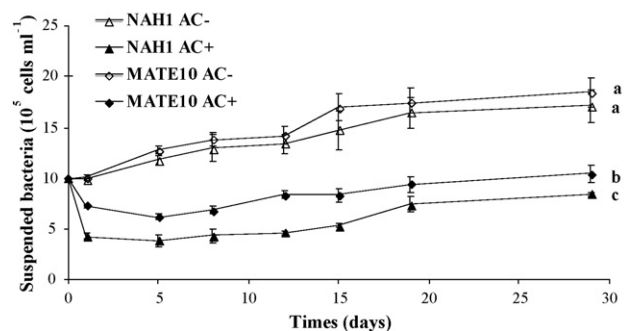


Fig. 4. Number of suspended bacteria with (AC+) or without (AC-) activated carbon during  $^{14}\text{C}$ -PHE mineralization by NAH1 or MATE10. Mean and standard error ( $n=3$ ). Different letters indicate significant difference ( $p \leq 0.05$ ) between treatments at the end of the experiment.

ation. Bacterial capacity to form biofilms might optimize PAH bioavailability by increasing diffusion coefficient through bio-surfactant effects, by increasing the interfacial area through biofilm surface and higher bacterial adhesion capacity. This hypothesis is supported by Van Dyke et al. [39] who have shown that *Pseudomonas aeruginosa* UG2 produced a rhamnolipid biosurfactant which improved the solubilization of hydrophobic compounds from soil. Addition of a rhamnolipid biosurfactant resulted in an increased mobilization of hexadecane [40], of PAH [13,41] and a transitory increase in phenanthrene mineralization rate [12,42]. Monitoring PHE distribution during incubation showed that the PHE concentration in solution and the total quantity of desorbed PHE were higher in treatment inoculated with NAH1, which formed biofilm, than with MATE10, which did not (Table 2). Bacterial adhesion to AC was observed for MATE10 and NAH1 during the first 5 days (Fig. 4). The higher adhesion of NAH1 on AC covered with PHE was observed in both experiments.

Hg porosimetry showed that AC porosity was mainly microporosity. Since bacterial mean size is around  $1 \mu\text{m}$  [43], only pores larger than  $1 \mu\text{m}$  would be accessible to bacteria. Pores with diameter greater than  $1 \mu\text{m}$  (Vb) represent 39 and 40% of ACPHE and AC porosity, respectively (Table 1). This suggests that the bacteria mainly had access to PHE adsorbed on AC external particle surface. Löser et al. [44] have found a stagnation of hydrocarbon biodegradation caused by a limited bioavailability of the pollutants due to the microporosity of an artificially contaminated sandy soil. The authors concluded that bioavailability of hydrocarbons was matrix-limited. This was not observed in present experiments.

## 5. Conclusion

Our results showed that five bacterial strains (NAH1, MATE3, MATE7, MATE10 and MATE12) isolated from PAH-contaminated soils with the same enrichment method differed in their capacity to degrade phenanthrene sorbed on activated carbon. Three of them (NAH1, MATE3 and MATE7) were able to degrade phenanthrene sorbed on activated carbon at higher rates than phenanthrene in solution. This may be due to their higher

adhesion capacity on activated carbon coated with phenanthrene and to the capacity to form biofilms.

## Acknowledgments

We thank the BRGM and ADEME for financial support.

## References

- [1] M. Alexander, Biodegradation and Bioremediation, vol. 1, Academic Press, San Diego, 1994.
- [2] J.J. Ortega-Calvo, C. Saiz-Jimenez, Effect of humic fractions and clay on biodegradation of phenanthrene by a *Pseudomonas fluorescens* strain isolated from soil, Appl. Environ. Microbiol. 64 (1998) 3123–3126.
- [3] M. Kästner, B. Mahro, Microbial degradation of polycyclic aromatic hydrocarbons in soils affected by organic matrix of compost, Appl. Microbiol. Biotechnol. 44 (1996) 668–675.
- [4] W.D. Weissenfels, H.J. Klewer, J. Langhoff, Adsorption of polycyclic aromatic hydrocarbons (PAHs) by soil particles: influence on biodegradability and biotoxicity, Appl. Microbiol. Biotechnol. 36 (1992) 689–696.
- [5] K. Nam, J.Y. Kim, Role of loosely bound humic substances and humin in the bioavailability of phenanthrene aged in soil, Environ. Pollut. 118 (2002) 427–433.
- [6] T.S. Poeton, H.D. Stensel, S.E. Strand, Biodegradation of polyaromatic hydrocarbons by marine bacteria: effect of solid phase on degradation kinetics, Water Res. 33 (1999) 868–880.
- [7] Y.M. Calvillo, M. Alexander, Mechanism of microbial utilization of biphenyl to polyacrylic beads, Appl. Microbiol. Biotechnol. 45 (1996) 383–390.
- [8] L. Bastiaens, D. Springael, P. Wattiau, H. Harms, R. De Wachter, H. Verachtert, L. Diels, Isolation of adherent polycyclic aromatic hydrocarbon (PAH)-degrading bacteria using PAH-sorbing carriers, Appl. Environ. Microbiol. 66 (2000) 1834–1843.
- [9] W.C. Tang, J.C. White, M. Alexander, Utilization of sorbed compounds by microorganisms specifically isolated for that purpose, Appl. Microbiol. Biotechnol. 49 (1998) 117–121.
- [10] M. Friedrich, R.J. Grosser, E.A. Kern, W.P. Inskeep, D.M. Ward, Effect of model sorptive phases on phenanthrene biodegradation: molecular analysis of enrichments and isolates suggests selection based on bioavailability, Appl. Environ. Microbiol. 66 (2000) 2703–2710.
- [11] H. Harms, A.J.B. Zehnder, Bioavailability of sorbed 3-chlorodibenzofuran, Appl. Environ. Microbiol. 61 (1995) 27–33.
- [12] M.A. Providenti, C.W. Greer, H. Lee, J.T. Trevors, Phenanthrene mineralization by *Pseudomonas* sp. UG 14, World J. Microbiol. Biotechnol. 11 (1995) 271–279.
- [13] K. Scheibenbogen, R.G. Zytner, H. Lee, J.T. Trevors, Enhanced removal of selected hydrocarbons from soil by *Pseudomonas aeruginosa* UG2 biosurfactants and some chemical surfactant, J. Chem. Technol. Biotechnol. 59 (1994) 53–59.
- [14] M. Eriksson, G. Dalhammar, W.W. Mohn, Bacterial growth and biofilm production on pyrene, FEMS Microbiol. Ecol. 40 (2002) 21–27.
- [15] K.K. Jefferson, What drives bacteria to produce a biofilm, FEMS Microbiol. Lett. 236 (2004) 163–173.
- [16] A.C. Rodrigues, S. Wuertz, A.G. Brito, L. Melo, Fluorene and phenanthrene uptake by *Pseudomonas putida* ATCC 17514: kinetics and physiological aspects, Biotechnol. Bioeng. 90 (2005) 281–289.
- [17] B. Guieysse, I. Bernhoft, B.E. Andersson, T. Henrysson, S. Olsson, B. Mattiasson, Degradation of acenaphthene, phenanthrene and pyrene in a packed-bed biofilm reactor, Appl. Microbiol. Biotechnol. 54 (2000) 826–831.
- [18] J. Rael, S. Shelton, R. Dayay, Permeable barriers to remove benzene: candidate media evaluation, J. Environ. Eng. 121 (1993) 411–415.
- [19] P. Leglize, A. Saada, J. Berthelin, C. Leyval, Evaluation of matrices for the sorption and biodegradation of phenanthrene, Water Res. 40 (2006) 2397–2404.
- [20] P. Binet, J.M. Portal, C. Leyval, Dissipation of 3–6 ring polycyclic aromatic hydrocarbons in the rhizosphere of ryegrass, Soil Biol. Biochem. 32 (2000) 2011–2017.
- [21] S.C. Corgié, T. Beguiristain, C. Leyval, Spatial distribution of bacterial communities and phenanthrene degradation in the rhizosphere of *Lolium perenne* L., Appl. Environ. Microbiol., in press.
- [22] S. Moller, A.R. Pedersen, L.K. Poulsen, E. Arvin, S. Molin, Activity and three-dimensional distribution of toluene degrading *Pseudomonas putida* in a multispecies biofilm assessed by quantitative *in situ* hybridization and scanning confocal laser microscopy, Appl. Environ. Microbiol. 62 (1996) 4632–4640.
- [23] J.H. De Boer, B.G. Lippens, J.C.P. Broekhoff, A. Van den Heuvel, T.J. Osinga, The *t*-curve of multimolecular N<sub>2</sub> adsorption, J. Colloid Interface Sci. 21 (1966).
- [24] K.S.W. Sing, D.H. Everett, R.A.W. Haul, L. Moscou, R.A. Pierotti, J. Rouquerol, et al., Reporting physisorption data for gas solid systems with special reference to the determination of surface-area and porosity (Recommendations 1984), Pure Appl. Chem. 57 (1985) 603–619.
- [25] H. Gaboriau, A. Saada, Influence of heavy organic pollutants of anthropic origin on PAH retention by kaolinite, Chemosphere 44 (2001) 1633–1639.
- [26] N. Amellal, J.M. Portal, J. Berthelin, Effect of soil structure on bioavailability of polycyclic aromatic hydrocarbons within aggregates of a contaminated soil, Appl. Geochem. 16 (2001) 1611–1619.
- [27] D.L. McNally, J.R. Mihelcic, D.R. Lueking, Biodegradation of mixtures of polycyclic aromatic hydrocarbons under aerobic and nitrate-reducing conditions, Chemosphere 38 (1999) 1313–1321.
- [28] E.V. Kozlova, I.F. Puntus, A.V. Slepkin, A.M. Boronin, Naphtalene degradation by *Pseudomonas putida* strains in soil model systems with arsenite, Process Biochem. 39 (2004) 1305–1308.
- [29] T.J. Cutright, S. Lee, Remediation of PAH-contaminated soil using *Achromobacter* sp., Energy Sources 16 (1994) 279–287.
- [30] S. Boochan, M.L. Britz, G.A. Stanley, Surfactant-enhanced biodegradation of high molecular weight polycyclic aromatic hydrocarbons by *Stenotrophomonas maltophilia*, Biotechnol. Bioeng. 59 (1998) 482–494.
- [31] A.L. Juhasz, G.A. Stanley, M.L. Britz, Microbial degradation and detoxification of high molecular weight polycyclic aromatic hydrocarbons by *Stenotrophomonas maltophilia* strain VUN 10,003, Lett. Appl. Microbiol. 30 (2000) 396–401.
- [32] P.B. Hatzinger, M. Alexander, Effect of aging of chemicals in soil on their biodegradability and extractability, Environ. Sci. Technol. 29 (1995) 537–545.
- [33] Y. Laor, P.F. Strom, W.J. Farmer, The effect of sorption on phenanthrene bioavailability, J. Biotechnol. 51 (1996) 227–234.
- [34] C. Moreno-Castilla, I.M.A.F.-G. Bautista-Toledo, J. Rivera-Utrilla, Influence of support surface properties on activity of bacteria immobilised on activated carbon for water denitrification, Carbon 41 (2003) 1743–1749.
- [35] S. Hwang, T.J. Cutright, Biodegradability of aged pyrene and phenanthrene in a natural soil, Chemosphere 47 (2002) 891–899.
- [36] N. Iwabuchi, M. Sunairi, M. Urai, C. Itoh, H. Anzai, M. Nakajima, S. Harayama, Extracellular polysaccharides of *Rhodococcus rhodochrous* S-2 stimulate the degradation of aromatic components in crude oil by indigenous marine bacteria, Appl. Environ. Microbiol. 68 (2002) 2337–2343.
- [37] S.L. Walker, The role of nutrient presence on the adhesion kinetics of *Burkholderia cepacia* G4g and ENV435g, Colloids Surf. B Biointerfaces 45 (2005) 181–188.
- [38] A.R. Johnsen, L.Y. Wick, H. Harms, Principles of microbial PAH-degradation in soil, Environ. Pollut. 133 (2005) 71–84.
- [39] M.I. Van Dyke, P. Couture, M. Brauer, H. Lee, J.T. Trevors, *Pseudomonas aeruginosa* UG2 rhamnolipid biosurfactant: structural characterization and their use in removing hydrophobic compounds from soil, Can. J. Microbiol. 39 (1993) 1071–1078.
- [40] D.C. Herman, R.J. Lenhard, R.M. Miller, Formation and removal of hydrocarbon residual in porous media: effect of attached bacteria and biosurfactant, Environ. Sci. Technol. 31 (1997) 1290–1294.



- [41] M.I. Van Dyke, S.L. Gulley, H. Lee, J. Trevors, Evaluation of microbial surfactants for recovery of hydrophobic pollutants from soil, *J. Ind. Microbiol.* 11 (1993) 163–170.
- [42] M.A. Providenti, C.A. Flemming, H. Lee, J.T. Trevors, Effect of addition of rhamnolipid biosurfactants or rhamnolipid-producing *Pseudomonas aeruginosa* on phenanthrene mineralization in soil slurries, *FEMS Microbiol. Ecol.* 17 (1995) 15–26.
- [43] B. Li, B.E. Logan, Bacterial adhesion to glass and metal-oxide surfaces, *Colloids Surf. B Biointerfaces* 36 (2004) 81–90.
- [44] C. Löser, H. Seidel, P. Hoffmann, A. Zehnsdorf, Bioavailability of hydrocarbons during microbial remediation of a sandy soil, *Appl. Microbiol. Biotechnol.* 51 (1995) 105–111.